Cell Reports Physical Science, Volume *4*

Supplemental information

Bioinspired and biomimetic cancer-cell-derived membrane nanovesicles for preclinical tumor-targeted nanotheranostics

Rajendra Prasad, Bárbara B. Mendes, Mahadeo Gorain, Gopal Chandra Kundu, Narendra Gupta, Berney Peng, Eaint Honey Aung Win, He Qing, and João Conde

Supplemental Information

Supplemental Experimental Procedures

Simulation. In this study, 3D model of gold nanorod was simulated with the finite element method (FEM) simulation software COMSOL Multiphysics (COMSOL; www.comsol.com) and COMSOL's RF Module. The dimensions of the AuNRs (Liposomes and CCMV supported gold nanorods) are 8.8 nm x 32.8 nm. The Perfectly matched layer, scattering boundary condition, perfect electric conductor, and perfect magnetic conductor, boundary conditions are applied. The electromagnetic field is 1e6 V/m. The AuNR with 3 nm lipid bilayer coating or CCMV bilayer coating was simulated, and the refractive index of coating were set to be 1.43 and 1.45. [S1, S2] The absorption peaks of nanorods with different coatings for the given direction of wave-vector 'k' of the electromagnetic field were evaluated. The amount of the absorbed light was determined using the cross-section calculation. [S3] The absorption cross-section of the particle, σ_{abs} can be calculated from the Poynting theorem as

$$\sigma abs = Wabs Sin \quad (1)$$

where S_{in} is the Poynting vector magnitude and where the power absorbed by the nanoparticle is

$$Wabs = \iiint VQhdV \quad (2)$$

Here, Q_h is defined as the total power dissipation density [W_{m3}] (i.e., the total losses of the system) based on the calculated EM fields. We obtained the total power absorbed by integrating over the volume, V, of the gold nanoparticle.[S4]

Blood circulation. We have followed earlier reported process[S5] to evaluate blood circulation of our designed nanotheranostics. Designed nanotheranostics particles were intravenously injected into tumor bearing female Balb/c mice. To check the presence of gold in blood, blood samples (25 µL from each) were collected at various time points for ICP-MS analysis. In brief, collected blood samples were treated with aqua regia for ICP-MS study.

Supplemental Figures

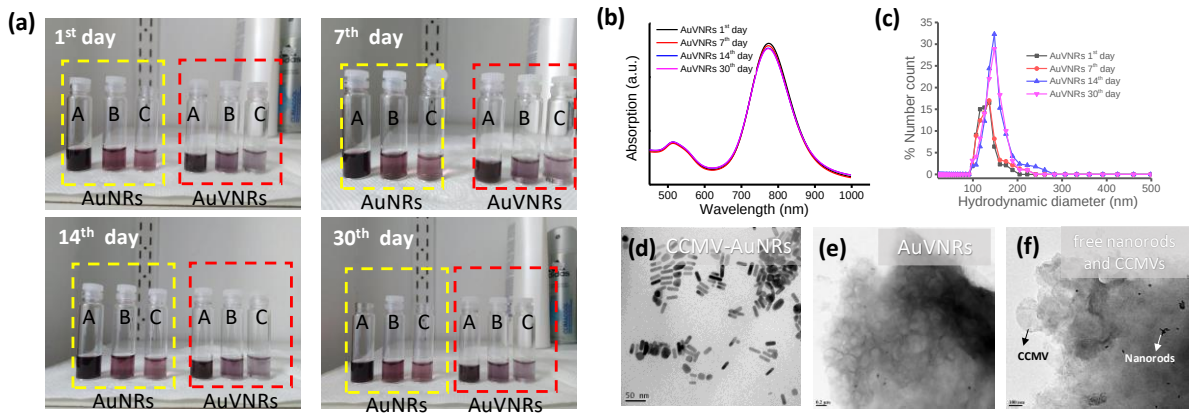

Fig. S1. Aqueous dispersion and stability of engineered nanoparticles. (a) Time dependent aqueous dispersion of AuNRs and AuVNRs. (b) Absorption spectra of AuVNRs at different time points (1, 7, 14 and 30th day). A - 0.5 mg. mL^{-1}; B - 0.25 mg. mL^{-1} and C – 0.125 mg. mL^{-1}. (c) Hydrodynamic diameters of AuVNRs in aqueous solution. TEM images (d) CCMV coated AuNRs, (e) purified AuVNRs and (f) free nanorods and CCMVs.

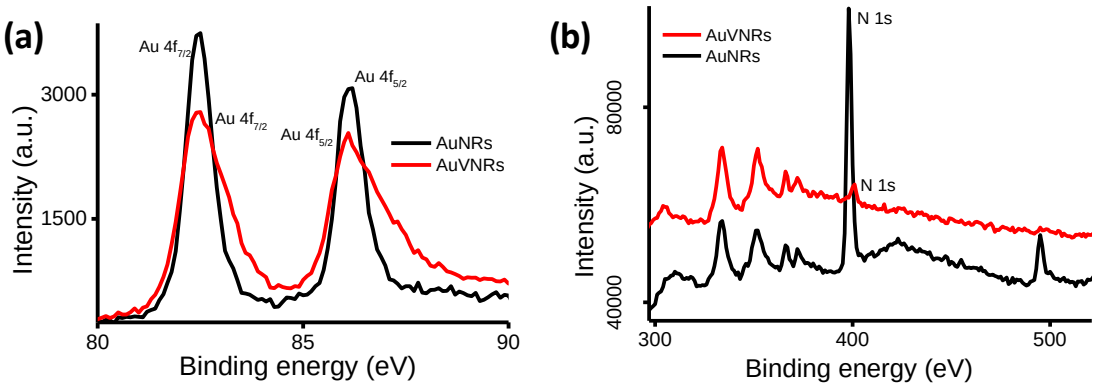

Fig. S2. XPS spectra of AuNRs and surface modified AuNRs (AuVNRs). Spectra showing characteristic (a) Au $4f_{7/2}$, Au $4f_{5/2}$ and (b) N 1s peak at 82.2, 86 and 400 eV respectively in both AuNRs and AuVNRs.

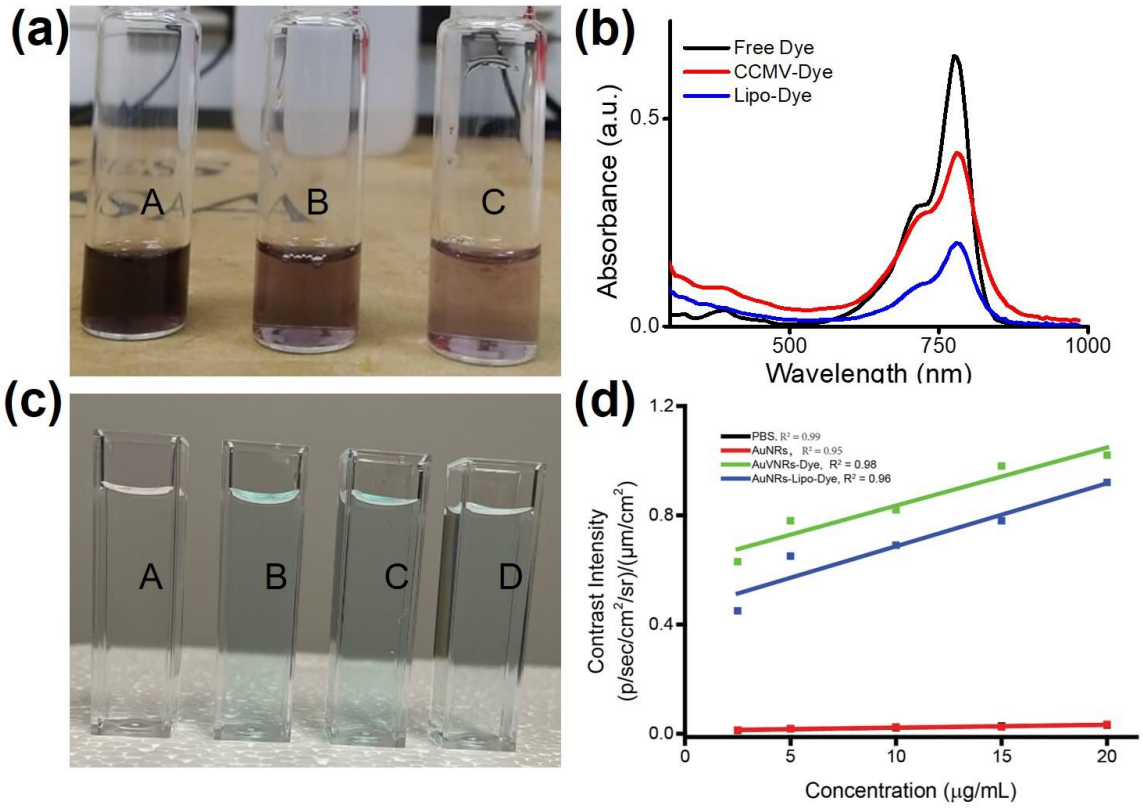

Fig. S3. ICG Dye-based nanoparticles absorption characterization. (a) Aqueous dispersion of the different nanostructures: A – AuNRs; B – AuVNRs-Dye and C – AuNRs-Lipo-Dye. (b) Absorption spectra and (c) Aqueous dispersion of the different nanostructures: A – PBS; B – Free Dye; C – CCMV-Dye, and D – Lipo-Dye. (d) Concentration dependent emissive response and linearity of AuNRs, AuVNRs-Dye and AuNRs-Lipo-Dye. R^2 value was 0.99 (PBS), 0.95 (AuNRs), 0.97 AuNRs-Lipo-Dye, and 0.98 (AuVNRs-Dye).

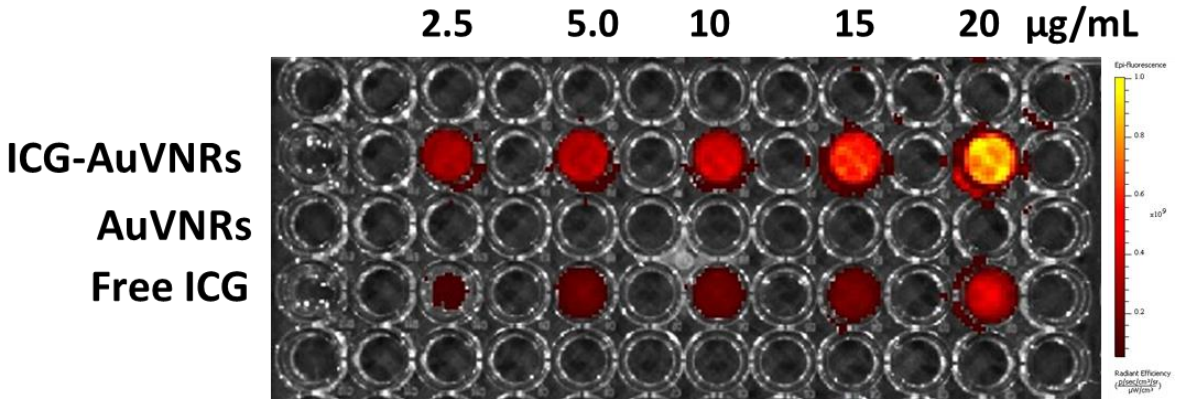

Fig. S4. Near infrared fluorescent characteristic of engineered nanotheranostic. Concentration dependent red emissive response of ICG dye encapsulated AuVNRs and comparison with free ICG dye.

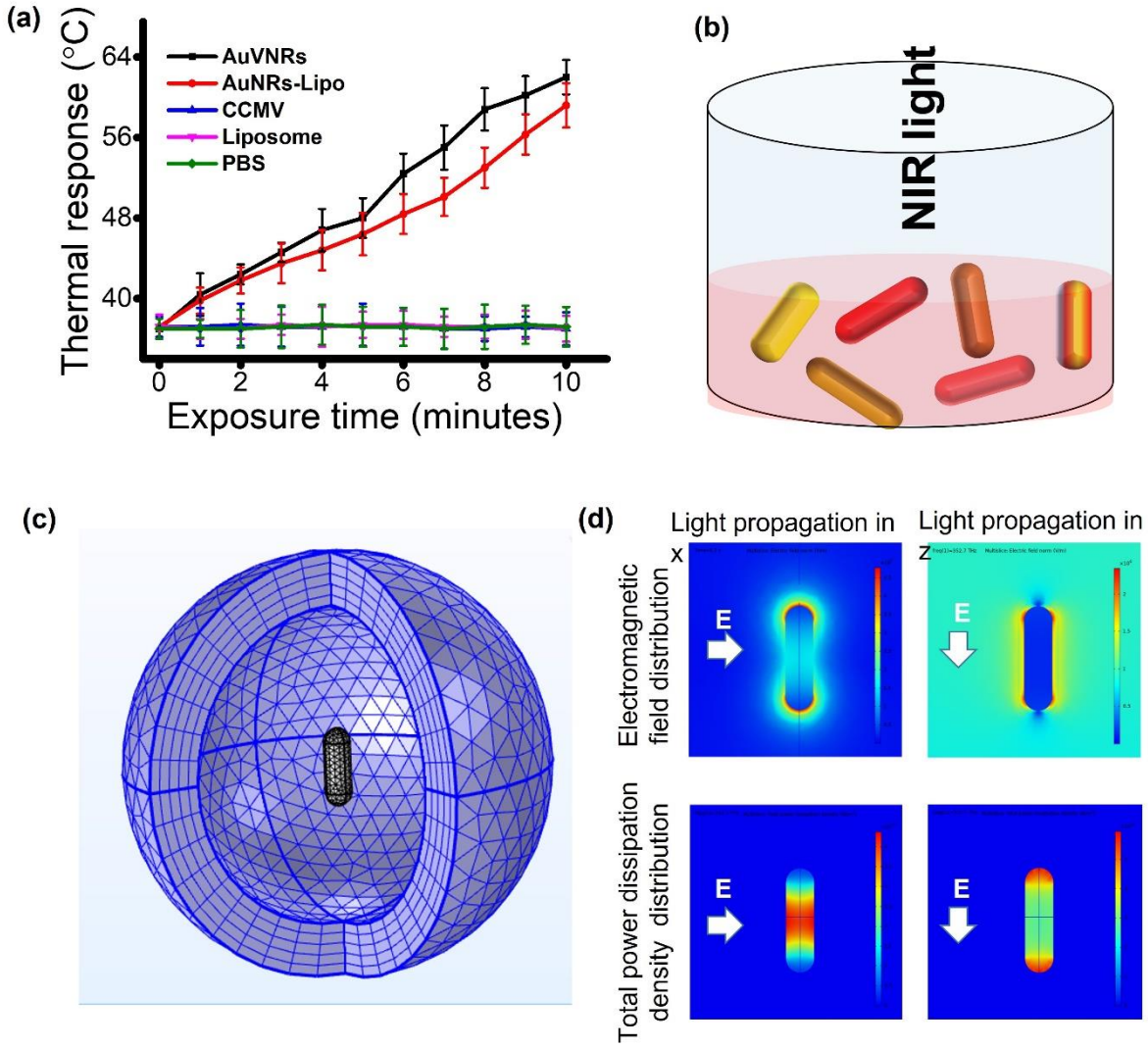

Fig. S5. Photo thermal response of studied nanostructures. (a) Time dependent photo thermal transduction of AuVNRs and AuNRs-Lipo using 800 nm NIR laser source (1 W power). (b) Depicted cartoon representing nanorod's thermal response under NIR exposure. (c, d) 3D model of simulated AuNRs using finite element method (FEM) simulation software COMSOL Multiphysics and COMSOL's RF Module.

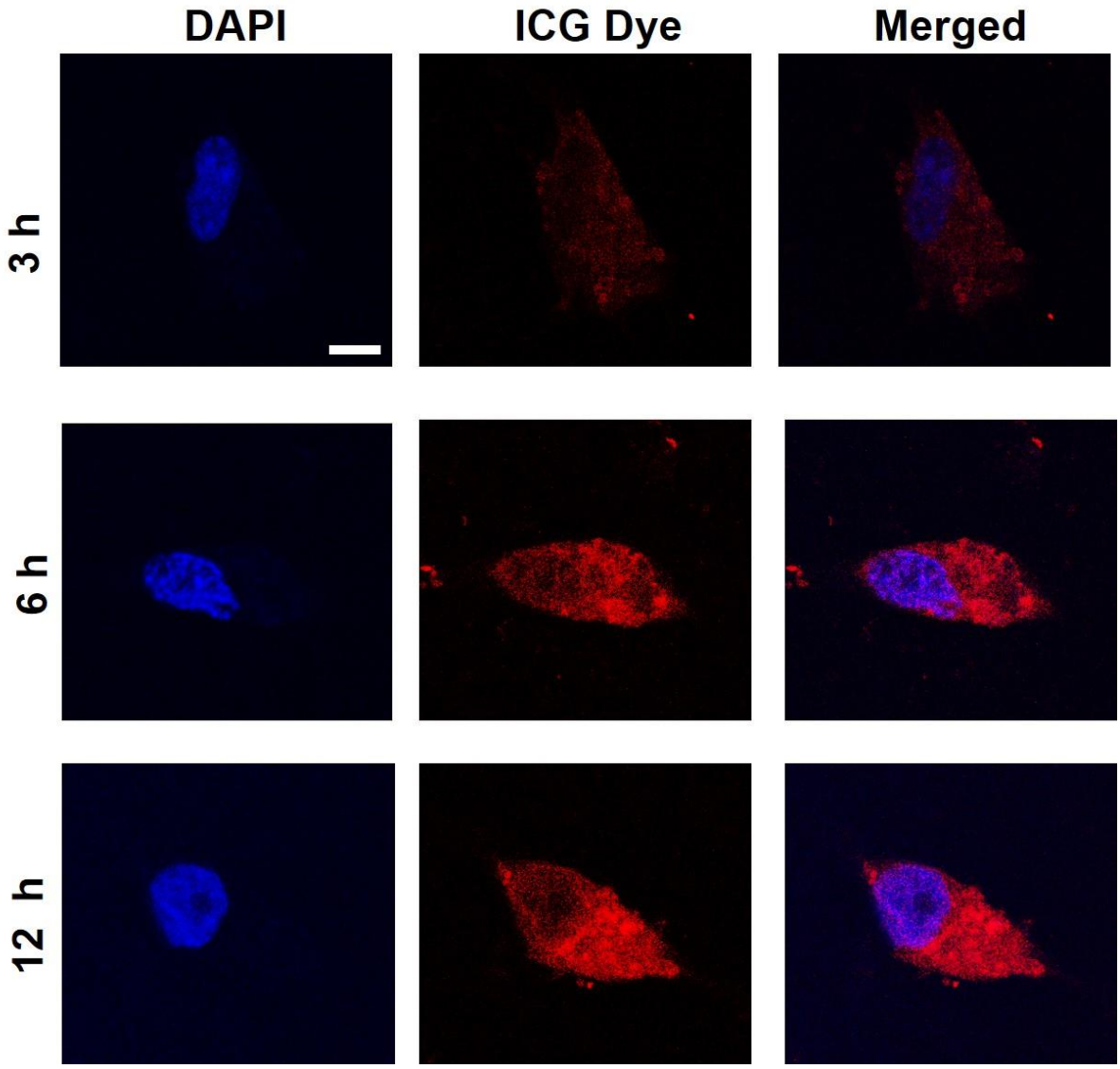

Fig. S6. Time dependent confocal images of AuVNRs-Dye for *in vitro* cancer cell targeting and uptake ability. Scale bar: 10 μm.

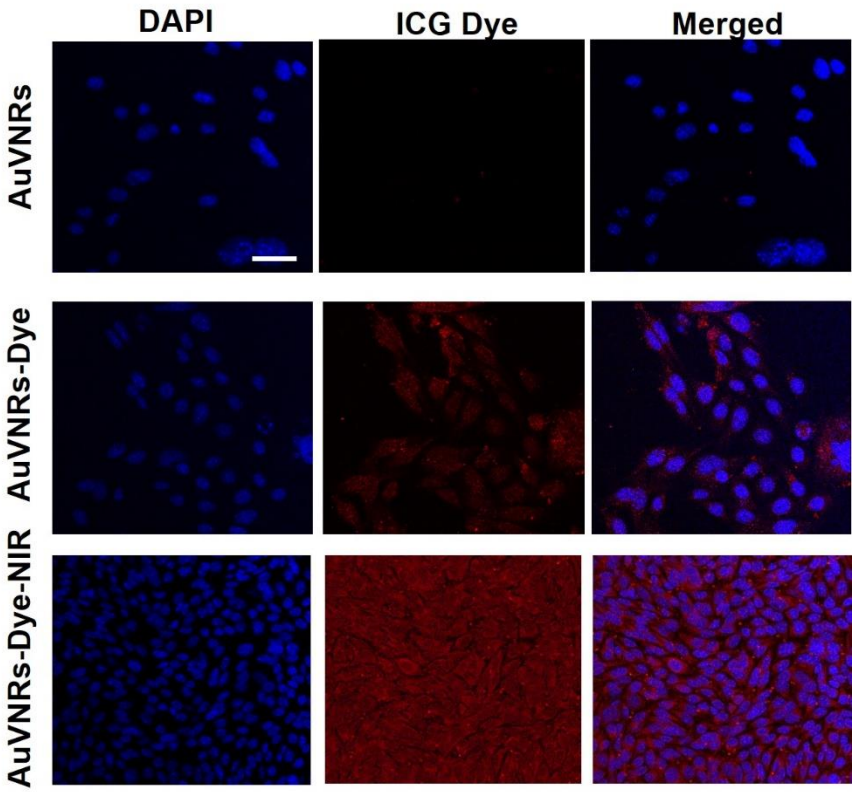

Fig. S7. *In vitro* cancer cell targeting and uptake ability. Confocal images of AuVNRs, AuVNRs-Dye with and without NIR light (800 nm, 1 W) exposure. Staining: DAPI (blue) and ICG dye (red). Scale bar: 50 μm.

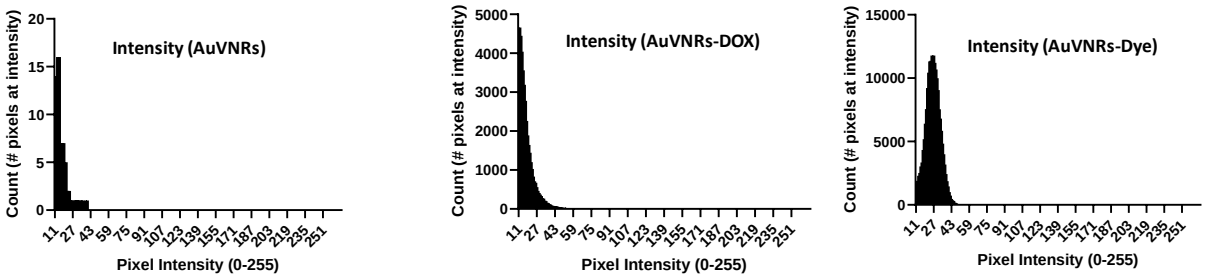

Fig. S8. *In vitro* pixel intensity analysis of cancer cell uptake ability of biomimetic ICG dye and DOX tagged theranostics system. The fluorescence intensity of 4T1 cells in the red channel.

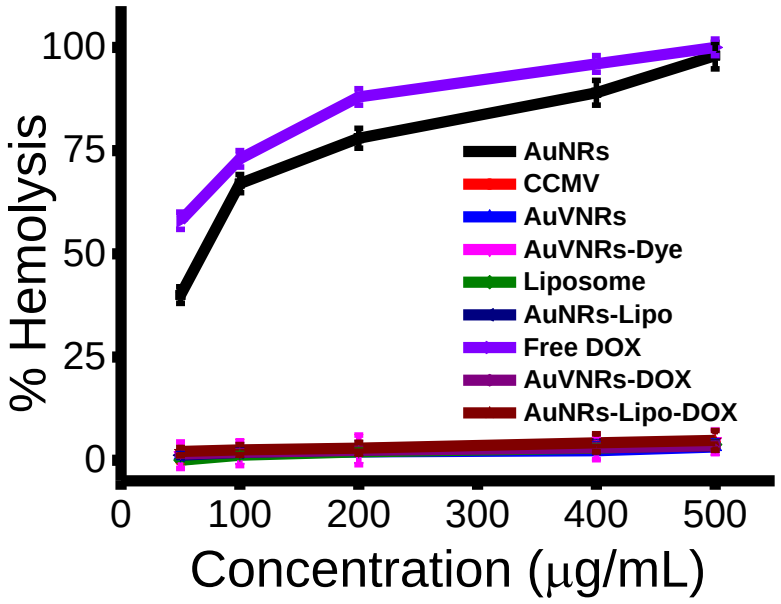

Fig. S9. Hemolysis observations with respect to concentrations (50-500 μg/mL) of prepared nanoformulations.

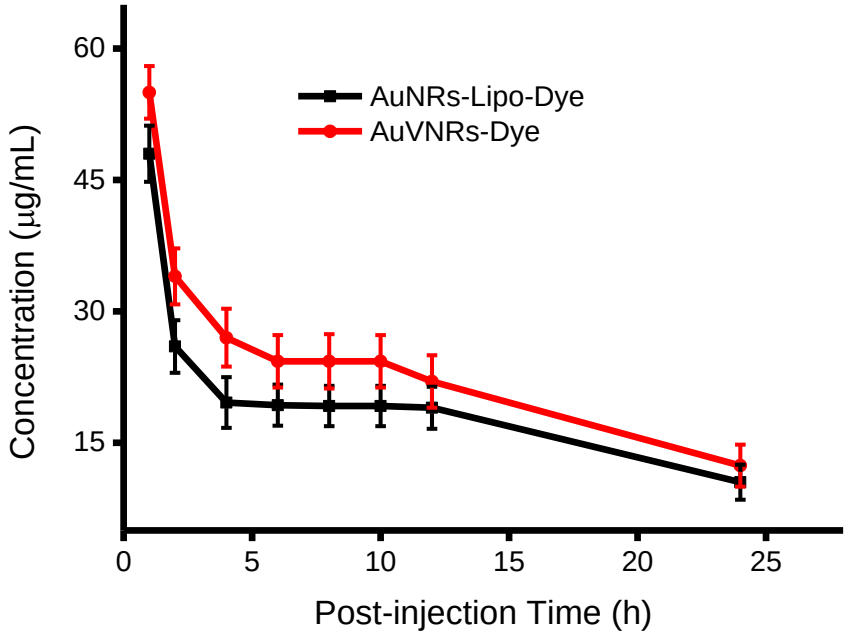

Fig. S10. Blood circulation lifetime of intravenously injected AuVNRs-Dye and AuNRs-Lipo-Dye, determined by inductively coupled plasma-mass spectrometry.

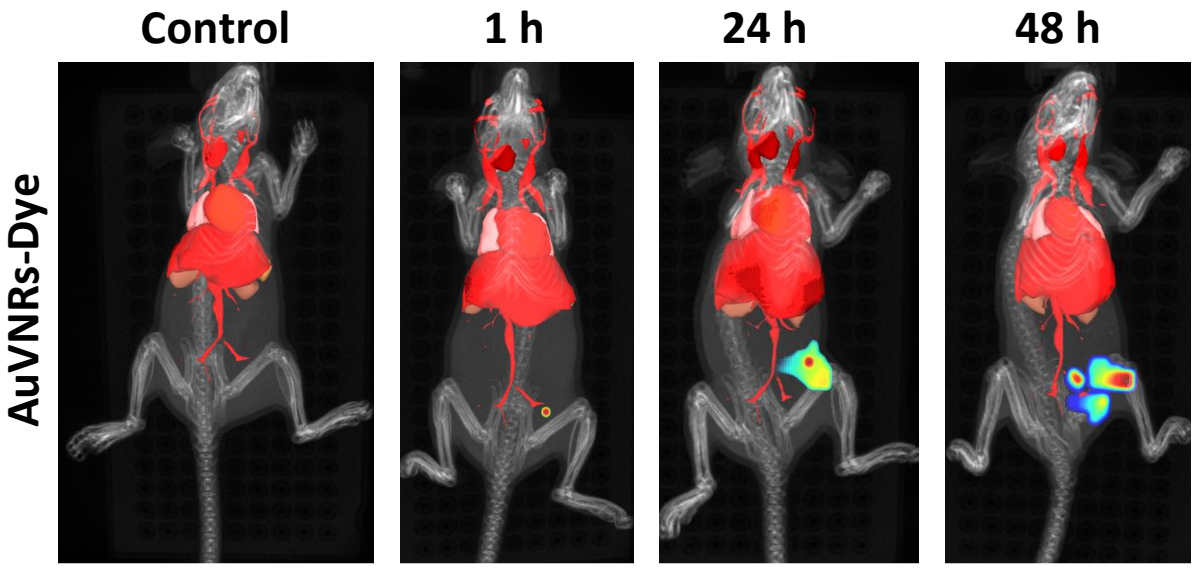

Fig. S11. Time-dependent tumor imaging after intravenously injected AuVNRs-Dye and compared with pre-injected animals (as control).

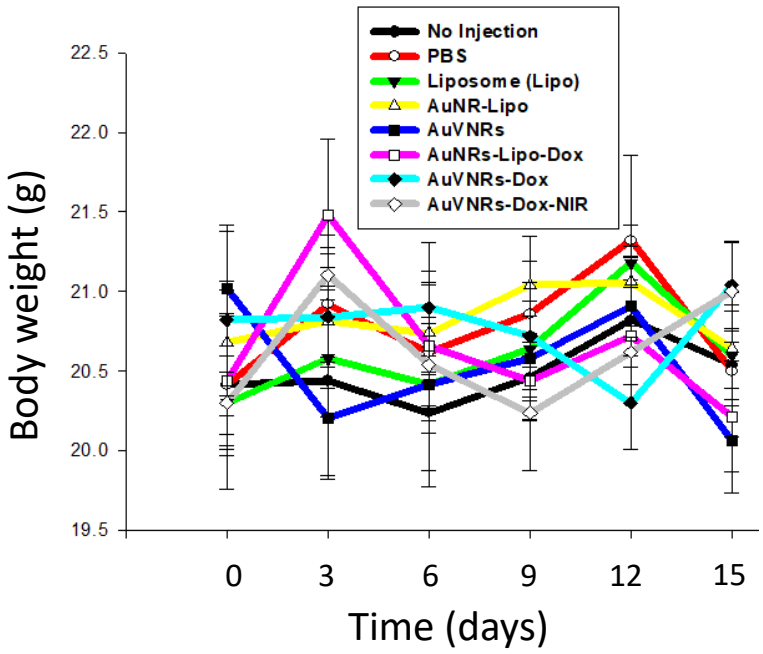

Fig. S12. Time dependent body weight measurements of AuVNRs, Liposomes, AuVNRs-DOX, AuVNRs-DOX under NIR, AuNRs-Lipo and AuNRs-Lipo-DOX treated tumor bearing mice and compared with control (pre-injected, as no injection and PBS treated animals).

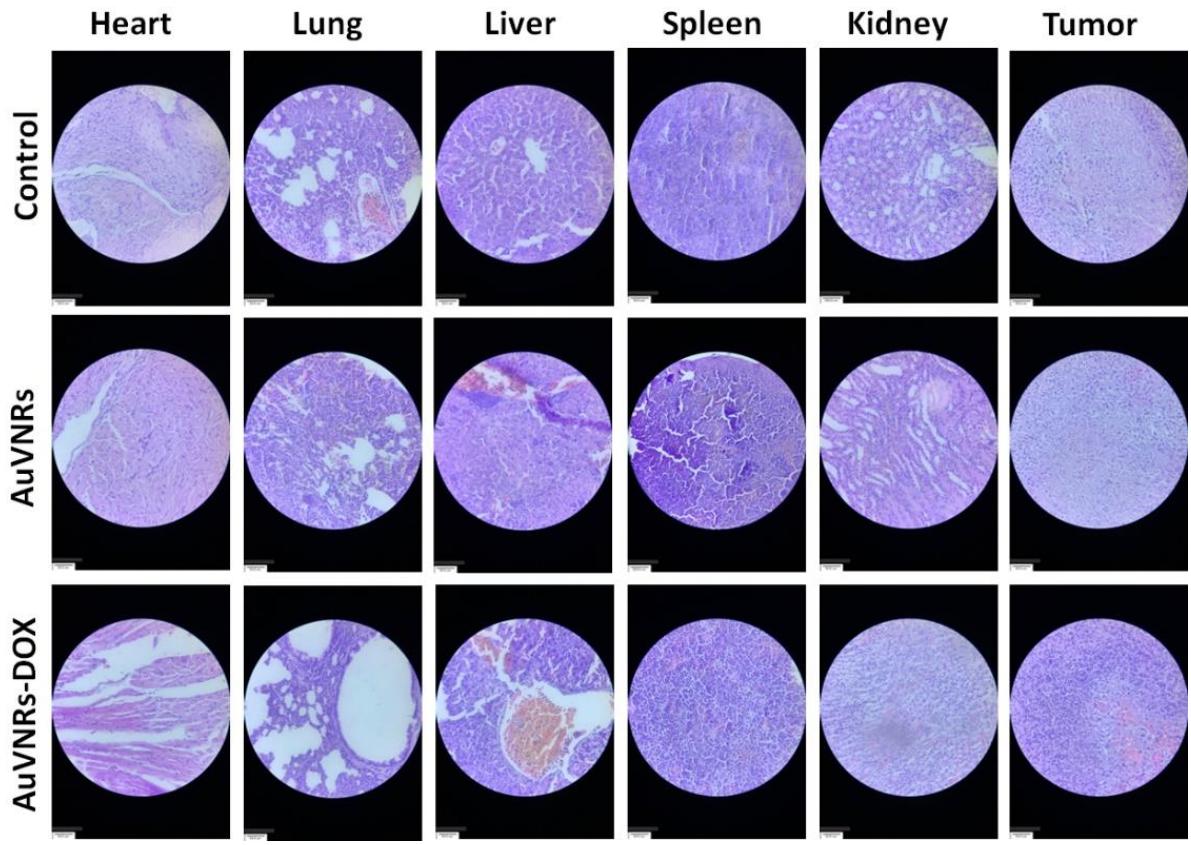

Fig. S13. Hematoxylin and Eosin (H&E) measurements of major organs collected from AuVNRs and AuVNRs-DOX treated mice and pre-injected mice (control). Scale bar: 50 µm.

Supplemental References

S1. Yu, Chenxu, and Joseph Irudayaraj. "Quantitative evaluation of sensitivity and selectivity of multiplex nanoSPR biosensor assays." *Biophysical journal* 93.10 (2007): 3684-3692.

S2. Ardhammar, Malin, Per Lincoln, and Bengt Nordén. "Invisible liposomes: refractive index matching with sucrose enables flow dichroism assessment of peptide orientation in lipid vesicle membrane." *Proceedings of the National Academy of Sciences* 99.24 (2002): 15313-15317.

S3. Bohren, Craig F., and Donald R. Huffman. *Absorption and scattering of light by small particles*. John Wiley & Sons, 2008.

S4. Manrique-Bedoya, Santiago, et al. "Multiphysics modeling of plasmonic photothermal heating effects in gold nanoparticles and nanoparticle arrays." *The Journal of Physical Chemistry C* 124.31 (2020): 17172-17182.

S5. Bindra, A.K., Sreejith, S., Prasad, R., Gorain, M., Thomas, R., Jana, D., Nai, M.H., Wang, D., Tharayil, A., Kundu, G.C. and Srivastava, R., A Plasmonic Supramolecular Nanohybrid as a Contrast Agent for Site-Selective Computed Tomography Imaging of Tumor. *Advanced Functional Materials*, 2022, 32(12), p.2110575.

S6. Dhiraj Kumar, Saikat Haldar, Mahadeo Gorain, Santosh Kumar, Fayaj A. Mulani, Amit S. Yadav, Lucio Miele, Hirekodathakallu V. Thulasiram and Gopal C. Kundu, Epoxyazadiradione suppresses breast tumor growth through mitochondrial depolarization and caspase-dependent apoptosis by targeting PI3K/Akt pathway. BMC Cancer 18, 52 (2018).